Available online at www.sciencedirect.com
SCIENCE DIRECT®
Catalysis Today 97 (2004) 103–112
CATALYSIS TODAY
www.elsevier.com/locate/cattod

Enhancement of the photo catalytic performance of TiO_2 catalysts via transition metal modification

Chun-Guey Wu*, Chia-Cheng Chao, Fang-Ting Kuo

Department of Chemistry, National Central University, Chung-Li, 32054 Taiwan, ROC

Received 18 November 2003; received in revised form 30 January 2004; accepted 5 April 2004
Available online 29 July 2004

Abstract

The physicochemical properties and photo catalytic activity of transition metal-loaded TiO_2 catalysts were studied. The transition metal was deposited on TiO_2 via post-hydrothermal synthesis and photo-assisted reduction/impregnation. The structure of TiO_2 is preserved upon adding Pd, Cr, and Ag into it. Nevertheless, the structure of TiO_2 was destroyed when reacted with silicotungstic acid (Si-W). As a consequence, under the irradiation of visible light, the Pd and Cr loaded TiO_2 showed higher photo catalytic activity compared to pristine TiO_2 and Si-W loaded TiO_2 has no catalytic activity, although the threshold absorptions of all metal loaded TiO_2 is similar to that of pure TiO_2. Transition metal was homogeneously coated on the TiO_2 particles and there is no phase separation between metal salts and TiO_2 as revealed with scanning electron micrographs (SEM), transmission electron microscopy (TEM) and X-ray diffraction (XRD) data. X-ray photoelectron spectroscopy (XPS) spectra showed that all metals in metal loaded TiO_2 presented as an ionic state with slightly reduction compared to the metal in metal salt used in the reaction, probably due to the interaction with TiO_2. These results suggested that the crystallinity was important for the photo catalytic activity of TiO_2 based catalysts and the function of transition metal is to increase the electron-hole recombination time, therefore increase the catalytic activity.

Keywords: Titanium oxide; Transition metal; Photo degrading; Organic waste

1. Introduction

TiO_2 is a low cost, radiation stable, non-toxic white pigment with broad applications in optical devices [1,2]. It is also a well-known, high band-gap semiconducting photosensitive material for photo anodes [3] and photo catalysts [4]. In fact, TiO_2 is famous with its high photo catalytic activity for the degradation of pollutant chemicals since reported by Frank in 1977 [5]. Nevertheless, TiO_2 uses only a very small fraction of the solar energy, due to its band-gap energy. A great effort was made to increase the activity of TiO_2 and reduce the band-gap energy to the visible light range. Furthermore, it was believed that the mechanism of photo activated catalytic reaction was via the formation of electron-hole pair, which reacted with the H_2O around to form OH radicals. The OH radical then degraded the organic wastes to smaller molecules or even CO_2 and H_2O. Therefore the photo catalytic activity of TiO_2 based catalysts can be improved by separation of the electron-hole pair to avoid the rapid recombination of electron and hole. It was know that doping with suitable transition metal ions allows extending the light absorption of large band-gap semiconductors to the visible region [6]. Furthermore, the transition metals or metal oxides (especial metals belonging to group VIII) were also proved to be an electron trapper, and therefore, avoiding the recombination of the electron-hole pairs of TiO_2 based catalysts [7–11]. In this article, the transition metal salts were added into the TiO_2 particles to increase the lifetime of the electron-hole pairs (besides to extend the light absorption to the visible region) and consequently, increase the photo catalytic activity.

* Corresponding author. Fax: +886 3 422 7664.
E-mail address: t610002@cc.ncu.edu.tw (C.-G. Wu).

0920-5861/$ – see front matter © 2004 Elsevier B.V. All rights reserved.
doi:10.1016/j.cattod.2004.04.055

2. Experimental section

2.1. Chemicals

$Ti(O\text{-}Pr)_4$, $HCl_{(aq)}$, $CH_3COOH_{(aq)}$, $H_2SO_{4(aq)}$, $H_2O_{2(aq)}$, $HNO_{3(aq)}$, $PdCl_2$, $Cr(NO_3)_3$, $AgNO_3$, $FeCl_3$, phosphomolybdic acid and silicotungstic acid hydrate were purchased from commercial resources and used without further treatment.

2.2. Preparation of TiO_2 particles

Two types of the TiO_2 particles TiO_2 sol and TiO_2 nano-crystallite were prepared via sol–gel and crystallization methods, respectively. $Ti(O\text{-}Pr)_4$ was used as Ti sources for both types of TiO_2 particles.

2.3. Sol–gel method for preparation of small (<20 nm) multi-crystalline TiO_2 sol

0.95 g of $Ti(O\text{-}Pr)_4$ was mixed well with 20 ml isoproponal, chilled in ice bath, then a chilled 180 ml, 0.03 M $HNO_{3(aq)}$ was added slowly into it with vigorous stirring. The mixture was stirred at ice bath for 4 h, kept in refrigerator for storage. Other reaction conditions were also used to synthesize TiO_2 sol and the reaction condition listed above can give the reproducible result with the TiO_2 particle less than 20 nm.

2.4. Crystallization method for preparation of single nanocrystals of TiO_2

9.25 ml of $Ti(O?\text{-}Pr)_4$ was mixed well with 2.5 ml of isoproponal, then added slowly into chilled acetic acid aqueous solution (v/v = 1:3). The mixture was stirred well and then loaded in an autoclave, heat at 80 °C for 8 h, then raises the temperature to 230 °C, heat for another 12 h. The titanium oxide-hydroxide gel obtained was dried at 50 °C to remove the water and side products. The solid was ground into a fine particle with an agate mortar and pestle. The nano-crystallites of TiO_2 were identified with X-ray powder diffraction and transmission electron microscopy (TEM) studies.

2.5. Preparation of metal-loaded TiO_2 sol and nano-crystallite

Two methods post-hydrothermal synthesis and photo-assisted reduction/impregnation, were use to synthesize metal-loaded TiO_2 sol and nano-crystallite.

2.6. Post-hydrothermal synthesis

A certain amount of transition metal salt was dissolved in water (or acidic solution), and then was mixed well with the TiO_2 sol (or TiO_2 nano-crystallites) suspended in water. The mole ratio of metal salt to Ti is 0.2, 0.1 or 0.05. The mixture was heated hydrothermally at 105 °C for 48 h. The solid was isolated by centrifugation, washing with water, and then drying in the oven. The presence of metal ion on the TiO_2 was confirmed with the ESCA spectra and the structure of the metal-loaded TiO_2 was identified with X-ray powder diffraction (XRD).

2.7. Photo-assisted reduction/impregnation [12–14]

A certain amount of transition metal salt was dissolved in water (or acidic solution), and then was mixed well with the TiO_2 sol (or TiO_2 nano-crystallites). The mole ratio of Ti to metal is 0.2, 0.1 or 0.05. The mixtures were irradiated with an UV light of wavelength ~365 nm for 48 h. After photo irradiation, the mixture solution was dried at 105 °C. The oxidation state of the metal and the structure of the metal-loaded TiO_2 were identified with ESCA spectra and X-ray powder diffraction pattern.

2.8. Photo catalytic activity of TiO_2-based catalysts

The catalytic activities of TiO_2 and its metal-loaded derivatives were investigated using the photo degrading of salicylic acid in water as test reactions. The experiments were carried out by mixing powder of TiO_2-based catalyst and salicylic acid aqueous solution in a glass container with a quartz lid, and irradiating with a 30 W high-pressure ultraviolet ($\lambda \sim 350$ nm) or 30 W mercury arc (wavelength > 300 nm) light in air. The decreasing of the concentration of the salicylic acid after reacting for 24 h was used to calculate the catalytic activities of TiO_2. The concentration of salicylic acid was monitored via its absorption intensity at 297 nm. Blank reactions (salicylic acid solution without TiO_2 catalyst and catalyst in pure water) were run in parallel to determine the background decomposition of salicylic acid by light and the absorption of the catalyst. The photo catalytic activity of the TiO_2 was evaluated as the amount of salicylic acid decomposed for 24 h irradiation at room temperature per gram of catalyst used.

2.9. Physicochemical measurements

UV–vis/NIR spectra were obtained using a Varian Cary 5E spectrophotometer in the laboratory atmosphere at room temperature. X-ray photoelectron spectroscopy studies were carried out on a Perkin-Elmer PHI-590AM ESCA/XPS spectrometer system with a cylindrical mirror electron (CMA) energy analyzer. The X-ray sources were Al Kα at 600 W. and Mg Kα at 400 W. X-ray diffraction studies were performed with a Shimadzu XRD-6000 X-ray diffractometer using Cu Kα radiation at 30 kV and 30 mA. Scanning electron micrographs (SEM) were recorded with a Hitachi S-800 at 15 kV. The samples for SEM imaging were mounted on metal stubs with a piece of conducting tape then coated with a thin layer of gold film to avoid charging. Transmission electron microscopy (TEM) was performed with a JEOL Jem-2000, FXII microscope at 120 kV.

Dynamic light scattering measurements of the TiO_2 particles were carried out with a Malvern Zetasizer 3000 laser light scattering spectrometer equipped with a He-Ne laser operated at λ_0 equal to 633 nm.

3. Results and discussion

3.1. Preparation of TiO_2

The Ti source used in the experiments is $Ti(O\text{-}Pr)_4$ and commercial Degussa P-25 (P-25) is used as a standard. The particle size of TiO_2 sol obtained from the sol–gel process depends on the experimental conditions. In general, big TiO_2 particles were obtained at lower acid concentration, higher water content and temperature. TiO_2 with particle sizes in the range of 10–2000 nm was prepared from different reaction conditions. However, a homogeneous clear sol solution exists only when the particle size is smaller than 200 nm and a white precipitate was formed when the average particle size is greater than 200 nm. X-ray powder diffraction pattern of TiO_2 sol showed predominantly the anatase phase (Fig. 1a). The crystalline domain size is much smaller than that of the size measured with a dynamic light scattering spectrometer, indicating that TiO_2 sol prepared from sol–gel process is not a well-defined single crystal. In fact, under TEM (Fig. 2a), the TiO_2 sol is a gel-like morphology composing a large amount of very small (<5 nm) TiO_2 crystallites. On the other hand, TiO_2 prepared from hydrothermal method is a single crystal with well-defined morphology (Fig. 2b). It is a pure anatase phase (Fig. 1b) and the crystal domain size calculated from the line broadening of X-ray diffraction pattern is similar to that obtained from TEM micrographs and dynamic light scattering measurements.

3.2. Synthesis of transition metal loaded TiO_2

Several transition metal salts, such as $PdCl_2$, $Cr(NO_3)_3$, $AgNO_3$, and $H_4SiO_4{\cdot}12WO_3{\cdot}xH_2O$ were used as the metal sources. Two preparation methods: post-hydrothermal synthesis and photo-assisted reduction/impregnation were used to incorporate transition metal in TiO_2. The purpose of post-hydrothermal synthesis was to incorporate metal ions in TiO_2 framework during the dissolving and re-crystallization process. On the other hand, the photo-assisted reduction/impregnation method was used to in situ reduction and deposition of metal ions on the surface of TiO_2.

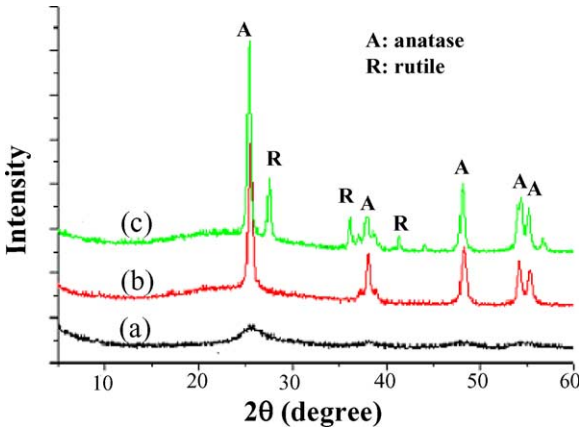

Fig. 1. The X-ray powder diffraction pattern of (a) TiO_2 sol, (b) TiO_2 nano-crystallite, (c) Degussa p-25.

3.3. Post-hydrothermal synthesis of metal-loaded TiO_2

Under TEM (Fig. 3), the morphology of metal-loaded TiO_2 sol is similar to that of pristine TiO_2 sol after post-hydrothermal treatment. Nevertheless, the SEM micrographs (Fig. 4) showed that after post-hydrothermal treatment, TiO_2 sol as well as Pd (or Ag)-loaded TiO_2 sol aggregated to bigger particles. The aggregation of Cr–TiO_2 is less serious and there is no aggregation of Si–W-loaded TiO_2 was observed, the surface morphology of Si–W-loaded TiO_2 film is much smoother than the others. Powder X-ray diffraction patterns (Fig. 5) of TiO_2 sol and metal-loaded TiO_2 sol showed that they are all only anatase phase

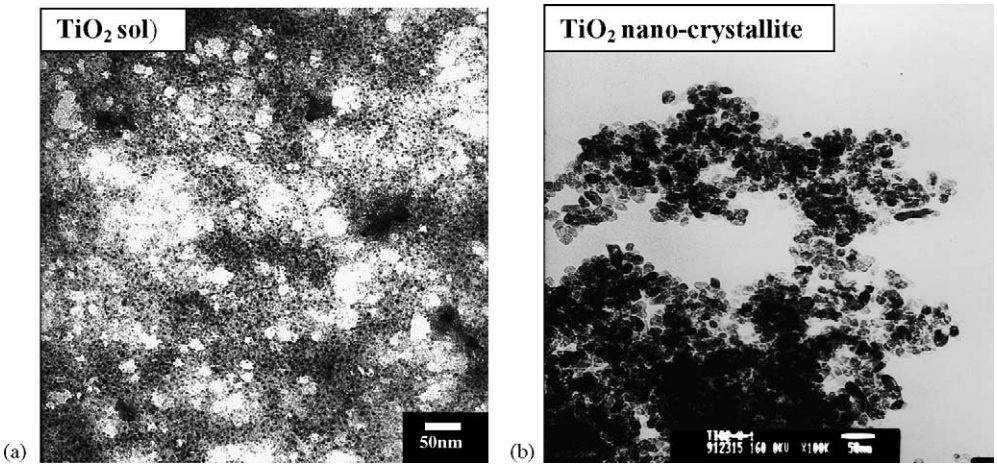

Fig. 2. TEM micrographs of (a) TiO_2 sol, (b) TiO_2 nano-crystallite.

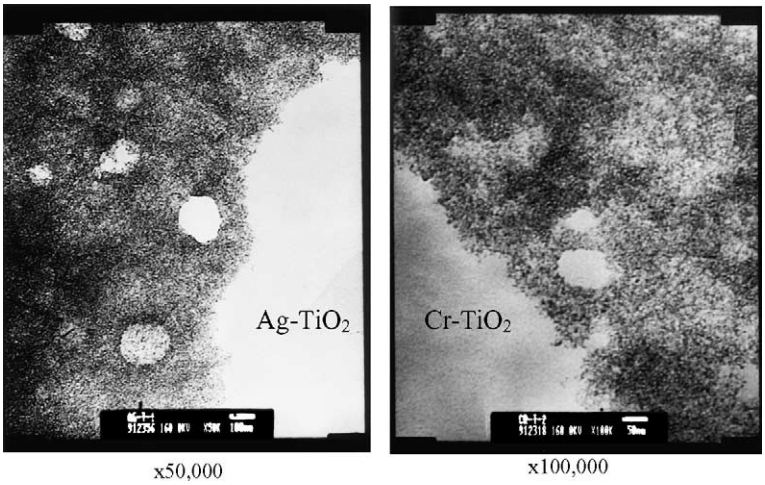

Fig. 3. TEM micrographs of metal-loaded TiO_2 sol.

with the crystalline domain size in the order of Ag–TiO_2 > hydrothermal treated TiO_2 sol ~ Cr–TiO_2 > Pd–TiO_2 > Si–W–TiO_2. Nevertheless, TEM, SEM micrographs and XRD data all revealed that there is no phase separation in metal-loaded TiO_2, suggesting that the metal salt was dispersed homogeneously on TiO_2 surface. On the other hand, the SEM graph and XRD pattern showed that the structure and morphology of TiO_2 nano-crystallite are preserved when the transition metal was added via post-hydrothermal synthesis, except Si–W–TiO_2 which the diffraction peaks of $H_4SiO_4{\cdot}12WO_3{\cdot}xH_2O$ was detected.

3.4. Photo-assisted reduction/impregnation of metal on TiO_2

The TEM and SEM micrographs of TiO_2 sol after photo-assisted reduction/impregnation of metal were very similar to those prepared via post-hydrothermal synthesis, except Si–W-loaded TiO_2. The morphology and crystallinity of TiO_2 changed when TiO_2 was mixed with $H_4SiO_4{\cdot}12WO_3{\cdot}xH_2O$ even at room temperature under stirring. X-ray diffraction pattern showed that the structure of TiO_2 was almost destroyed and a new peak belongs to the crystalline $H_4SiO_4{\cdot}12WO_3{\cdot}xH_2O$ appeared at low 2θ angle in Si–W-loaded TiO_2. TEM micrographs of TiO_2 nano-crystallites after photo-assisted reduction/impregnation of metals were shown in Fig. 6. It seems that the TiO_2 nano-crystallites grow bigger and more dispersed after the metal salts were added. Similar conclusion can be made from the SEM studies (Fig. 7) with the exception of Si–W-loaded TiO_2. SEM of Si–W-loaded showed that the TiO_2 grains were buried inside the $H_4SiO_4{\cdot}12WO_3{\cdot}xH_2O$ matrix. XRD pattern (Fig. 8) revealed that the crystallinity of TiO_2 nano-crystallites was intact when the metal was added, except Si–W-loaded TiO_2 which the structure of TiO_2 is also almost totally destroyed. EDS analysis showed the presence of both transition metal and Ti in metal loaded TiO_2 and there is no phase separation was observed from the SEM, TEM and X-ray diffraction data.

3.5. Photo catalytic activities of TiO_2 based catalysts

A simple comparison among the results obtained from the different preparation and modification methods (or reported in the literature) for metal-loaded TiO_2 is almost impossible. It is due to that catalysts prepared under different experimental conditions are usually different. For example, it is well known that bare crystalline anatase and rutile TiO_2 show very different photo catalytic activity, depending on their electronic and surface properties [15]. Therefore, the activity of TiO_2 based catalysts cannot be straightforwardly related to only a few properties because it depends on all of them. We compare the activity of TiO_2 based catalysts using the same batch of TiO_2 as starting materials. The mechanism of photo catalytic degrading of organic compounds is believed to involve absorption of an UV photo by TiO_2 to produce an electron-hole pair. Both hole and electron can react with water to yield hydroxyl and superoxide radicals which oxidize the organic molecules. The ultimate products of these reactions are CO_2 and water [16–18]. The photo-decomposed products of salicylic acid are also CO_2 and H_2O; therefore, the amount of salicylic acid decomposed can be monitored by the decreasing of the absorption intensity of salicylic acid at 297 nm.

The photo catalytic activities of metal-loaded TiO_2 sol obtained from post-hydrothermal synthesis of TiO_2 sol under the illumination of UV and Hg arc light are listed in Table 1. It was founded that the photo catalytic activity of all metal-loaded TiO_2 under the illumination of UV light is worse than that of hydrothermal treated TiO_2, except Ag–TiO_2. It is probably due to that some active sites were hindered by the transition metal therefore decreased the activity and the higher activity of Ag–TiO_2 is due to its good crystallinity and good electron trapping effect of Ag ions and

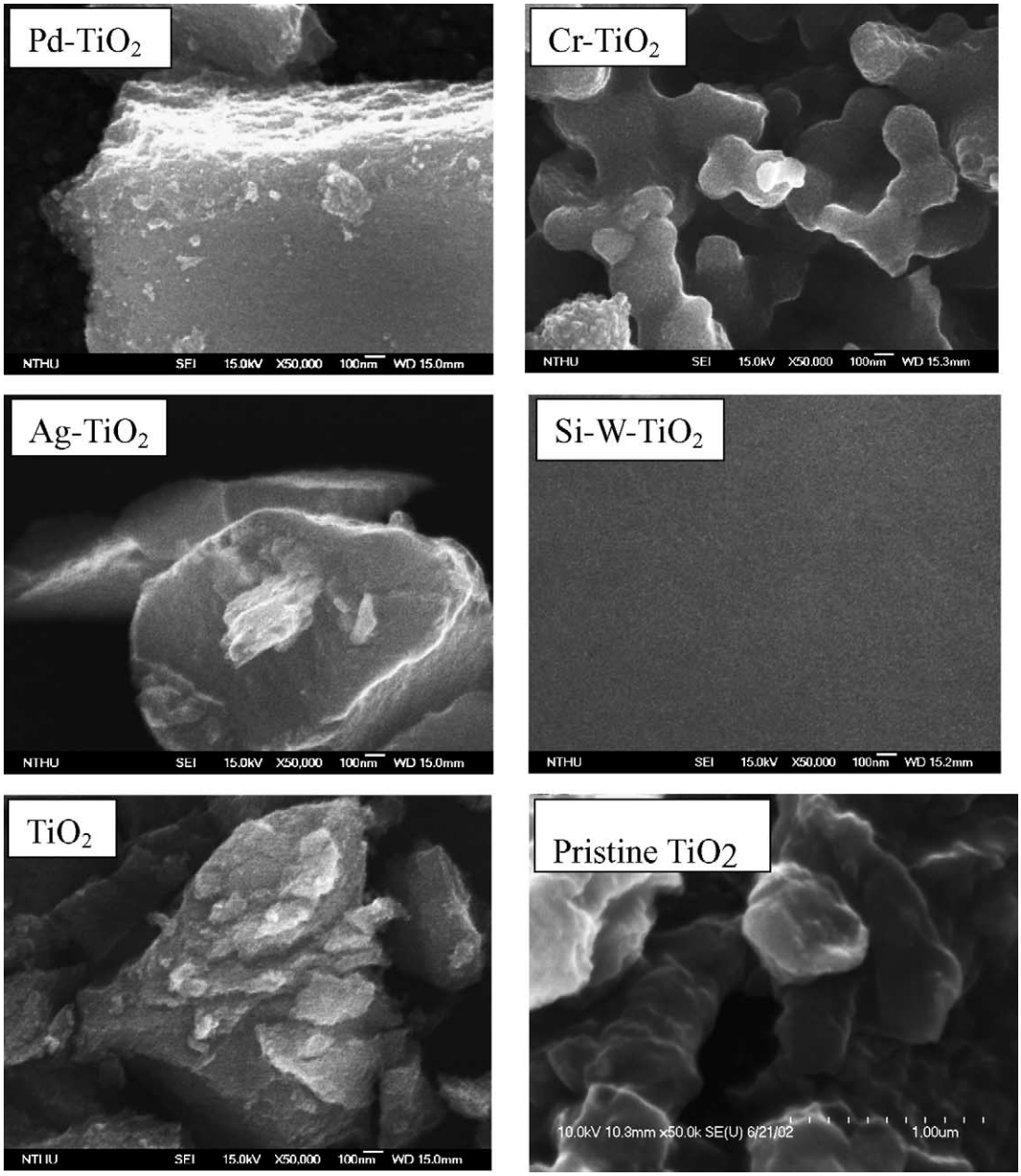

Fig. 4. SEM micrographs of TiO_2 sol and metal-loaded TiO_2 sol prepared from post-hydrothermal synthesis (magnification: 50,000×).

Table 1
The color, absorption threshold wavelength and catalytic activity of metal-loaded TiO_2 prepared from TiO_2 sol using post-hydrothermal method

Catalyst[a]	Color	Absorption threshold (nm)	Catalytic activity under UV light (mmole)[b]	Catalytic activity under Hg arc light (mmol)
TiO_2	White	363	4.06	0.24
Pd–TiO_2	Brown	367	2.19	0.9
Cr–TiO_2	Green	386	2.86	0.57
Ag–TiO_2	Gray	354	4.64	0.39
Si–W–TiO_2	Pale yellow	378	1.29	0.20
Degussa p-25	White	343	5.36	~0

[a] The mole ratio of the metal to TiO_2 is 0.1.
[b] The activity was represented as mmole of salicylic acid decomposed per gram of TiO_2 for 24 h reaction.

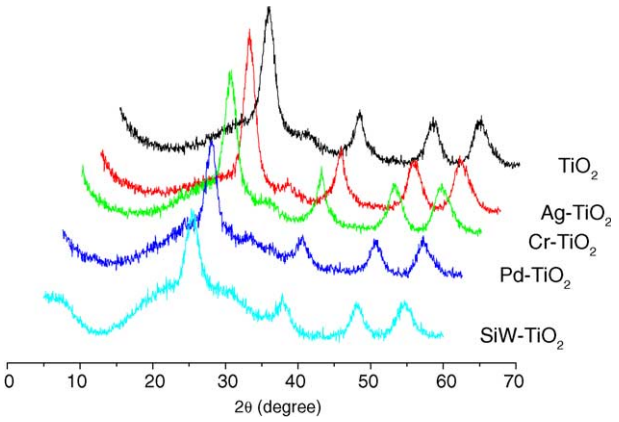

Fig. 5. X-ray powder diffraction patterns of TiO_2 sol and metal-loaded TiO_2 sol prepared from post-hydrothermal synthesis.

may be also the low absorption threshold. Nevertheless, under the illumination of the visible light, the catalytic activity of all metal-loaded TiO_2 is better than that of hydrothermal treated pure TiO_2 sol although all catalysts showed lower activity compared to those under the irradiation of UV light. This is probably due to that the absorption threshold is still in the UV range.

Loading transition metal in TiO_2 has two possible effects: extending the absorption spectra of the TiO_2 into the visible region and avoiding the electron-hole recombination by electron trapping. Both effects will increase the catalytic activity when the reactions were carried out under the irradiation of the visible light. However, when the reactions were carried out under the irradiation of UV light, the former effect will be negative. The data in Table 1 showed that the

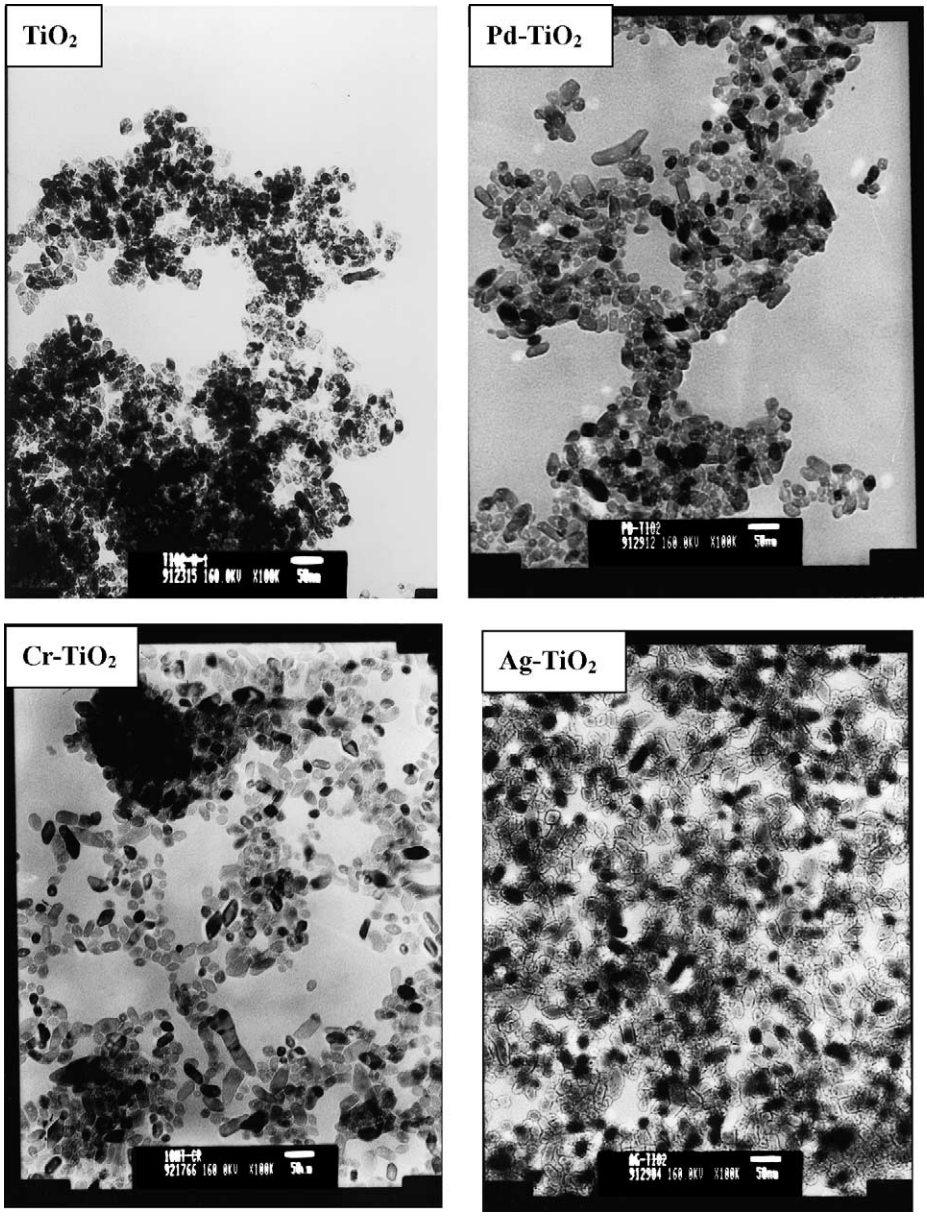

Fig. 6. TEM micrographs of TiO_2 nano-crystallite and metal-loaded TiO_2 nano-crystallite prepared from photo-assisted reduction/impregnation (magnification: 1,00,000×).

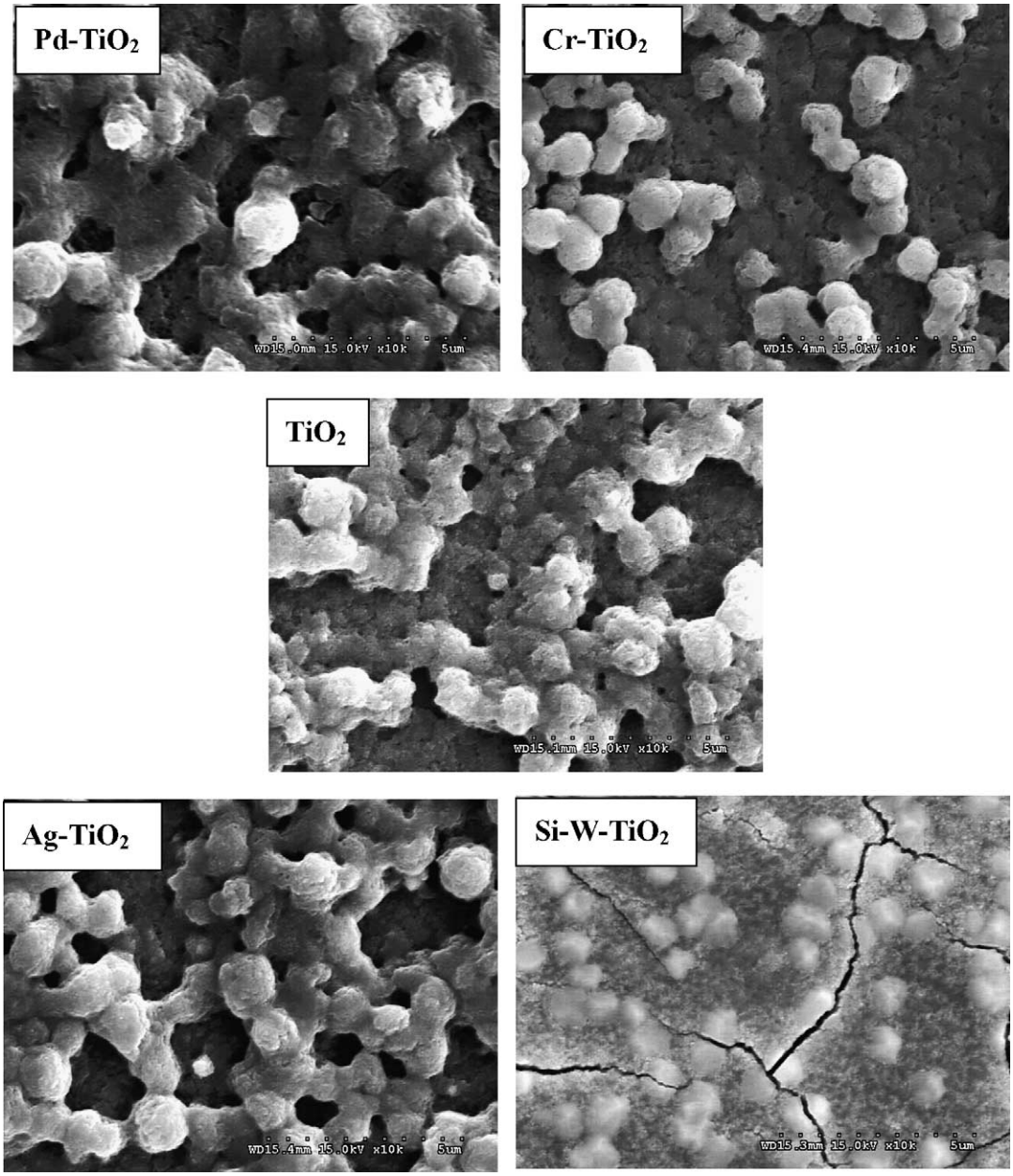

Fig. 7. SEM micrographs of TiO_2 nano-crystallite and metal-loaded TiO_2 nano-crystallite prepared from photo-assisted reduction/impregnation (magnification: 1,00,00×).

enhanced catalytic activity for Cr–TiO_2 and Pd–TiO_2, under the irradiation of the visible light, is due to the extending of the absorption spectra of metal-loaded TiO_2 into the visible region. For Ag–TiO_2 which absorption threshold shifted to low wavelength, the enhanced activity is due to the electron trapping effect that can be proved from the activity data when the reactions were carried out under the UV lighting. Under the irradiation of UV light (the absorption threshold of TiO_2-based catalysts is not so important), Ag^+ acts as a good electron trapper, therefore Ag–TiO_2 has a slowest electron-hole recombination rate and highest catalytic activity amongst all metal-loaded TiO_2 catalysts with the same metal to TiO_2 ratios.

One of the major proposes for the modification of TiO_2 based photo catalysts was to increase their activity under the irradiation of sun light. Therefore, the catalytic activities of TiO_2-based catalysts prepared from different source and methods under the Hg arc (visible) light were studied and the results are summarized in Table 2. In general, the activity of Pd–TiO_2 has the highest catalytic activity under all experiment conditions we had used. However, the photo catalytic activity of Ag–TiO_2 varied with preparation conditions. It was known [19] that adding Fe(III) to TiO_2 can increase its activity on the photodecomposition of phenol in water. Palmisano and coworkers [20]. prepared TiO_2 powders loaded with transition metal ions by using the incipient

Table 2
The catalytic activity (under the illumination of Hg arc light) of metal loaded TiO_2 prepared with various methods

Catalyst[a]	Preparation method			
	TiO_2 sol, post-hydro-thermal	TiO_2 sol, photo-assisted reduction	TiO_2 nano-crystallite, post-hydro-thermal	TiO_2 nano-crystallite, photo-assisted reduction
	Activities[b]			
TiO_2	0.24	0.36	0.64	0.73
Pd–TiO_2	0.9	1.1	0.87	0.98
Cr–TiO_2	0.57	0.83	0.81	0.95
Ag–TiO_2	0.39	0.75	0.41	0.36
Si–W–TiO_2	0.20	~0	0.10	~0

[a] The mole ratio of metal to Ti is 0.1.
[b] The activity was represented as mmol of salicylic acid decomposed during 24 h per gram of TiO_2.

wet impregnation method and found that the photo catalytic activity of TiO_2 was reduced by the presence of transition metal ions with the exception of W, which instead played a beneficial role. Ag metal had been proved to be a good additive for the photodecomposition of urea [21] and 2-propanol [22] when TiO_2 was used as a catalyst. Those results are not totally consistent with what we had observed. What are all these contradictions come from? What are the factors, except the components, which determine the activity of TiO_2-based photo catalysts? The following few paragraphs may provide some cues.

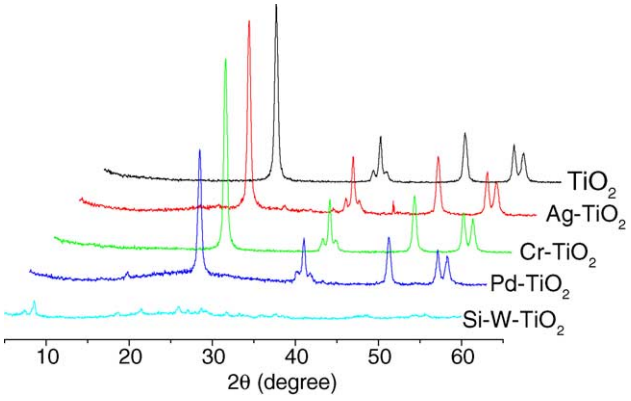

Fig. 8. X-ray powder diffraction patterns of TiO_2 nano-crystallite and metal-loaded TiO_2 nano-crystallite prepared from photo-assisted reduction/impregnation.

3.6. Catalytic activity related physicochemical properties of the metal-loaded TiO_2

X-ray diffraction patterns revealed that, besides Si–W–TiO_2 which the anatase phase of TiO_2 destroys totally, all metal-loaded TiO_2 showed a pure anatase phase with various crystalline domain sizes. The crystalline domain size versus activity of TiO_2 and metal-loaded TiO_2 was shown in Fig. 9. It was found that only crystalline TiO_2 has catalytic activity. Amorphous TiO_2 may have different band structure and density of states compared to crystalline TiO_2, therefore, showed no photo catalytic activity. Nevertheless, the activity is not directly related to the crystalline domain size. Some

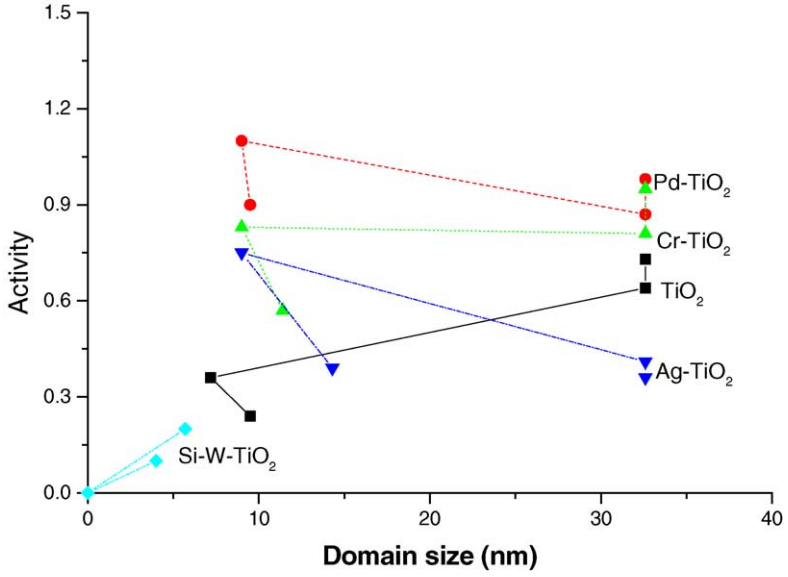

Fig. 9. The catalytic activity vs. crystallinity of TiO_2 and metal-loaded TiO_2 prepared from various methods.

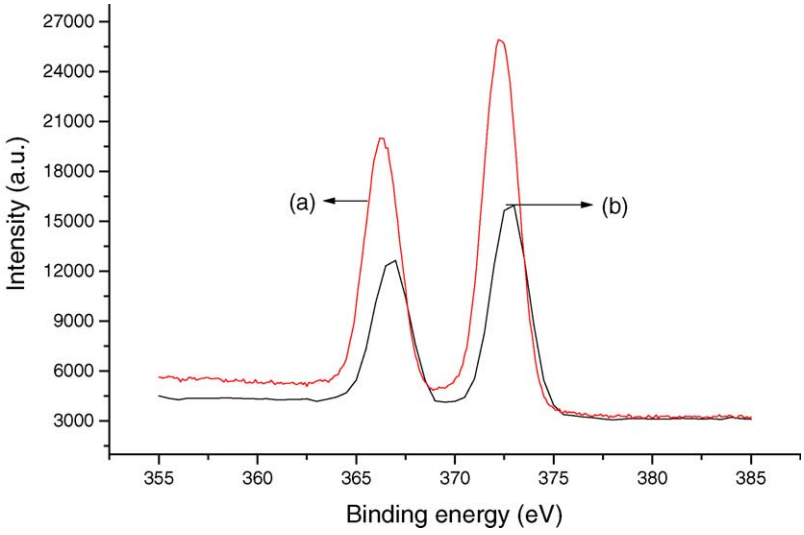

Fig. 10. XPS spectra of Ag in Ag–TiO_2 nano-crystallite prepared from (a) post-hydrothermal synthesis, (b) photo-assisted reduction/impregnation.

other parameters, such as the oxidation state of metal, may be also involved. The papers reported by Papp et al. [13], Albert et al. [14], and Schiavello et al [23]. showed that the transition metal in metal-loaded TiO_2 prepared from the photo-assisted reduction/impregnation presents as an element form for Pd and Ag and oxides for Cr. It will be useful to know the oxidation state of the metal in metal-loaded TiO_2 used in this study. The representative X-ray photoelectron spectroscopy (XPS) spectra of metal-loaded TiO_2 nano-crystallite prepared with our methods were shown in Fig. 10 and the binding energy and full-width-half-maximum (FWHM) were summarized in Table 3. The binding energy of Pd is 1–2 eV higher than that of Pd^0 and lower than that in $Pd^{2+}Cl_2$ [24]. The result indicated that the Pd presents as an ion form with partial reduction or interaction with the oxygen in TiO_2. The UV irradiation did not cause the significant reduction of Pd ion, contrasting to what Papp and Albert had observed. On the other hand, Pd in the post-hydrothermal synthesized Pd–TiO_2 nano-crystallite has a lower binding energy compared to that prepared from photo-assisted reduction/impregnation method. This result suggested that Pd in hydrothermally prepared Pd–TiO_2 has a higher degree of reduction compared to that in Pd–TiO_2 synthesized with photo-assisted reduction/impregnation method. Similar phenomenon was also observed in Ag–TiO_2 and Cr–TiO_2. Combination the catalytic activity data shown in Table 2, it seems that in Ag–TiO_2, Ag with lower oxidation state will have a higher activity but in Pd–TiO_2 and Cr–TiO_2 the higher activity was found when the oxidation state of Pd and Cr is higher. Furthermore, the FWHM of Pd in Pd–TiO_2 prepared with post-hydrothermal method is much wider than that obtained from photo-assisted reduction method, indicating Pd in Pd–TiO_2 prepared hydrothermally has more complicated chemical environment. Nevertheless, the FWHM of Ag and Cr in metal-loaded

Table 3
The binding energy and FWHM of metal-loaded TiO_2 nano-crystallite

Preparation method	Element	Binding energy (eV)	FWHM (eV)
Post-hydrothermal	Pd	336	3.18
	Cr	576.5	3.64
	Ag	367	2.25
Photo-assisted reduction	Pd	337	2.29
	Cr	577	3.71
	Ag	367.5	2.15

Table 4
The catalytic activity (under the illumination of Hg arc light) of metal-loaded TiO_2

Catalyst[a]	Preparation method	Mole ratio of metal to TiO_2[b]	Activity[c]
Cr–TiO_2	Photo-assisted reduction	0.2	0.80
		0.1	0.95
		0.05	0.60
	Post-hydrothermal	0.2	1.10
		0.1	0.81
		0.05	0.52
Ag–TiO_2	Photo-assisted reduction	0.2	0.07
		0.1	0.36
		0.05	0.14
	Post-hydrothermal	0.2	0.17
		0.1	0.41
		0.05	0.22
Pd–TiO_2	Photo-assisted reduction	0.1	0.98
	Post-hydrothermal	0.1	0.87
TiO_2	TiO_2 nano-crystallite, photo-assisted reduction	0	0.73

[a] TiO_2 nano-crystallite was used as a source.

[b] The mole ratio of metal to TiO_2 is the mole ratio of metal salt to TiO_2 in the reaction media. Due to the different work-out procedure, the mole ratio of metal to TiO_2 of the catalysts prepared from photo-assisted reduction method is the same as that in the reaction media. Nevertheless, the mole ratio of metal to TiO_2 in the catalysts prepared from post-hydrothermal method may be different from that in the reaction media.

[c] The activity was represented as mmole of salicylic acid decomposed during 24 h per g of TiO_2.

Table 5
The binding energy and FWHM of metal-loaded TiO_2 nano-crystallite

Preparation method	Element	Binding energy (eV)	FWHM (eV)
Post-hydrothermal	Pd	336	3.18
	Cr	576.5	3.64
	Ag	367	2.25
Post-hydrothermal	Pd	336	3.18
	Cr	577	3.71
	Ag	367.5	2.15

TiO_2 prepared with post-hydrothermal method is close to that synthesized from photo-assisted reduction/impregnation. This may imply that the interactions between Ag (or Cr) and TiO_2 are very weak. The oxidation state of the metals and the interactions between metal and TiO_2 in metal-loaded TiO_2 will have a large impact on their catalytic activity. Detailed studies on the synthesis of metal-loaded TiO_2 with controllable metal oxidation states and their XPS spectra are under way.

The metal concentration may also have an obviously effect on the activity of the metal-loaded TiO_2 catalysts. The activity of metal-loaded TiO_2 with various metal contents was listed in Table 4. From the previous discussion, we know that there are so many parameters that will affect the photo catalytic activity of TiO_2 based catalysts, the data shown in Table 4 had proved that the metal concentration is one of them. To explore the effect of the metal concentration on the catalytic activity of metal-loaded TiO_2 catalysts, other parameters, such as particle size, crystallinity, preparation method, homogeneity of metal dispersion, and so on should be fixed. In this respect, metal-loaded TiO_2 prepared from the photo-assisted reduction/impregnation of TiO_2 nano-crystallite is a good system to study. The data in Table 4 showed that there is an optimal metal concentration to achieve the highest activity. If the concentration of metal is too low, the effect will not be significant. For high metal content catalyst, the active sizes of TiO_2 will be blocked, therefore the catalytic activity decreased. These results suggested that the photo catalytic activity of transition metal loaded TiO_2 was determined at least by two parameters: the amount of metal and the active sites of the TiO_2. The optimal compositions depend on the types of metal and the preparation methods (Table 5).

4. Conclusion

Transition metals were deposited on TiO_2 via post-hydrothermal synthesis and photo-assisted reduction/impregnation methods. X-ray photoelectron spectroscopy data showed that the transition metal presents as an ion form with some interactions with TiO_2. The photo catalytic activity of metal-loaded TiO_2 is better than pristine TiO_2 sol under the irradiation of the visible light. It seems that the crystallinity of TiO_2, the absorption threshold, the interaction between metal ions and TiO_2, and the type, the oxidation state, and the concentration of the metal as well as the irradiation source have an impact on the catalytic activity of metal-loaded TiO_2 photo catalysts. Under the irradiation of the visible light, Pd–TiO_2 has the highest activity amongst all the metal-loaded TiO_2 studied in the article. This may due to that Pd ion has a strongest interaction with TiO_2.

Acknowledgements

Financial support of this work by the Chinese Petroleum Company (Grant No.: NSC-89-CPC-7-008-008) and National Science Council of the Republic of China is gratefully acknowledged.

References

[1] B.E. Yoldas, T.W. O'Keefe, Appl. Opt. 18 (1979) 3133.
[2] M. Lottiaux, C. Boulesteix, G. Nihoul, F. Varnier, F. Flory, R. Galindo, E. Pelletier, Thin Solid Films 170 (1989) 107.
[3] A. Fujishima, K. Honda, Nature 238 (1972) 37.
[4] M.R. Hoffmann, S.T. Martin, W. Choi, D.W. Bahnemann, Chem. Rev. 95 (1995) 69.
[5] S.N. Frank, J. Am. Chem. Soc. 99 (1977) 4667.
[6] M. Anpo, Catal. Surv. Jpn. 1 (1997) 169.
[7] W. Lee, Y.M. Gao, K. Dwight, A. Wold, Mater. Res. Bull. 27 (1992) 685.
[8] A. Sclafani, M.N. Mozzanega, P.J. Pichat, Photochem. Photobiol. A Chem. 59 (1991) 181.
[9] W. Lee, Y.R. Do, K. Dwight, A. Wold, Mater. Res. Bull. 28 (1993) 1127.
[10] T. Carlson, G.L. Griffin, J. Phys. Chem. 90 (1986) 5896.
[11] S. Ikeda, N. Sugiyama, B. Pal, G. Marci, L. Palmisano, H. Noguchi, K. Uosaki, B. Ohtani, Phys. Chem. Chem. Phys. 3 (2001) 267.
[12] J. Gimenez, M.A. Aguado, S. Cerveramarch, J. Mol. Catal. A Chem. 105 (1996) 67.
[13] J. Papp, H.S. Shen, A. Heller, K. Dwight, A. Wold, Chem. Mater. 5 (1993) 284.
[14] M. Albert, Y.M. Gao, D. Toft, K. Dwight, A. Wold, Mater. Res. Bull. 27 (1992) 961.
[15] A. Sclafani, L. Palmisano, M. Schiavello, J. Phys. Chem. 94 (1990) 829.
[16] L. Spanel, M.A. Anderson, J. Am. Chem. Soc. 113 (1991) 2628.
[17] S. Goldstein, G. Czapski, J. Rabani, J. Phys. Chem. 98 (1994) 6586.
[18] R.W. Mathews, J. Catal. 97 (1987) 565.
[19] E.C. Butler, A.P. Davis, J. Photochem. Photobiol. A: Chem. 70 (1993) 273.
[20] A.Di. Paola, G. Marci, L. Palmisano, M. Schiavello, K. Uosaki, S. Ikeda, B. Ohtani, J. Phys. Chem. 106 (2002) 637.
[21] M. Kondo, W.F. Jardin, Water Res. 25 (1991) 823.
[22] A. Sclafani, M.N. Mozzanega, P. Pichat, J. Photochem. Photobiol. A Chem. 59 (1991) 181.
[23] M. Schiavello, Electrochim. Acta 38 (1993) 11.
[24] J. Chastain, R.C. King (Eds.), Handbook of X-ray Photoelectron Spectroscopy. Physical Electronics, Inc., 1992.